ISSN 1070-3284, Russian Journal of Coordination Chemistry, 2022, Vol. 48, No. 1, pp. 1–8. © Pleiades Publishing, Ltd., 2022.
Russian Text © The Author(s), 2022, published in Koordinatsionnaya Khimiya, 2022, Vol. 48, No. 1, pp. 3–10.

Study of Cationic Porphyrins and Their Metal Complexes by ESR Techniques

N. E. Sannikova[a], K. A. Zhdanova[b], A. S. Spitsyna[a, c], N. A. Bragina[b], M. V. Fedin[a, *], and O. A. Krumkacheva[a, **]

[a] *International Tomography Center, Siberian Branch, Russian Academy of Sciences, Novosibirsk, Russia*
[b] *MIREA–Russian Technological University, Moscow, Russia*
[c] *Vorozhtsov Novosibirsk Institute of Organic Chemistry, Siberian Branch, Russian Academy of Sciences, Novosibirsk, Russia*
**e-mail: mfedin@tomo.nsc.ru*
***e-mail: olesya@tomo.nsc.ru*

Received April 30, 2021; revised June 29, 2021; accepted July 30, 2021

Abstract—The cationic *meso*-aryl-substituted porphyrins and their metal complexes were studied as model compounds for photodynamic therapy by electron spin resonance (ESR) techniques. Symmetrical cationic porphyrins with terminal pyridinium groups on short alkyl spacers and their Zn(II) and Cu(II) complexes were synthesized. Zero-field splitting parameters of the photoexcited triplet states were determined by time-resolved ESR. For Cu(II) complexes, the hyperfine coupling between the paramagnetic ligand and the nitrogen atoms of the porphyrin ring was measured. The effect of pyridinium substituents and the ligand on the magnetic-resonance parameters of porphyrins was analyzed on the basis of the obtained results.

Keywords: porphyrins, zinc complexes, synthesis, ESR spectroscopy
DOI: 10.1134/S1070328422010031

INTRODUCTION

Porphyrin derivatives play an important role in various photochemical and photobiological processes taking place in nature. The amphiphilic meso-aryl-substituted porphyrins and their metal complexes are of considerable interest for medical applications [1–3]. These compounds possess specific properties: high molar absorption coefficients, relatively high triplet state and fluorescence quantum yields; the complex formation with paramagnetic metals gives rise to the use of porphyrins in medicine as active compounds in radiological [4] and magnetic resonance [5] diagnosis of cancer and as photosensitizers in the photodynamic therapy (PDT) of cancer [6–8].

It is known that minor changes in porphyrin structures can induce changes in their physicochemical properties and, hence, in the scope of their applicability [9]. Such transformations were successfully used to develop several active and selective biomimetic catalytic systems and to develop contrast agents used in medical visualization, PDT, and antimicrobial photodynamic therapy (APDT) [10]. In addition, some photosensitizers (PS) that belong to this group of molecules are already present in the pharmaceutical market and have been approved for clinical use [11].

In view of the prospects of *meso*-aryl-substituted porphyrins as PS, study of the properties of their triplet states is a relevant task. Another important issue is to study the role of ligands and porphyrin structure for binding to biomolecules [12]. It is assumed that the ligand changes the geometric structure of the porphyrin, making the porphyrin ring more or, conversely, less planar, which affects the degree of DNA binding [13]. Measurement of the hyperfine coupling between the paramagnetic ligand and the nitrogen atoms of the porphyrin central ring provides information on the geometry of the porphyrin core and on the structural changes caused by the introduction of ligands and substituents.

Time-resolved ESR (TR ESR) is a direct method for detection of short-lived radicals and triplet molecules [14–16]. The method is based on the excitation of molecules of the sample with laser radiation and subsequent recording of the time evolution of the magnetization signal in an invariable magnetic field. The ESR spectral pattern of the triplet state is determined by the splitting parameters of the triplet sublevels (D and E) in a zero magnetic field and by relative occupancies of these sublevels (Scheme 1, Fig. 1). It is known that parameters D and E depend on the structure of the photosensitizer and the nature of the central metal [17–19]. Comparison of these data for various PS allows one to gain information about the change in the spatial distribution of spin density and the triplet state symmetry [17–19].

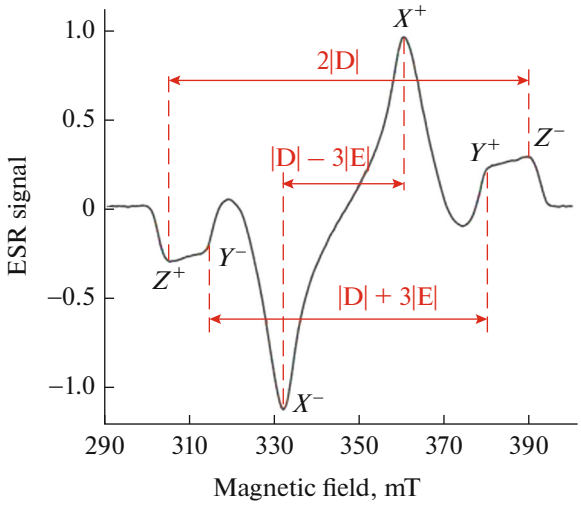

Fig. 1. Characteristic TR ESR spectra of the triplet state with designation of parameters D and E.

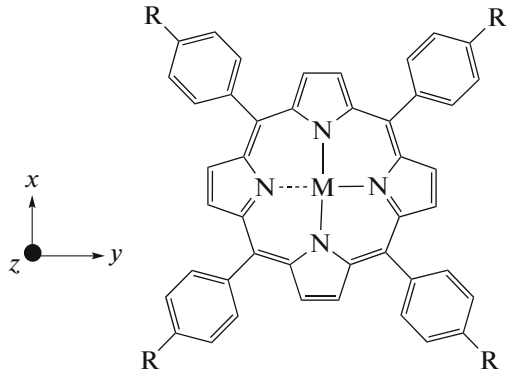

Scheme 1.

Therefore, in this study, we synthesized new symmetrical cationic porphyrins with terminal pyridinium groups on short alkyl spacers and their Zn(II) and Cu(II) complexes. The effect of pyridinium substituents and Zn(II) ions on the magnetic resonance parameters of photoexcited triplet porphyrins was studied by the TR ESR method. For Cu(II) complexes, the hyperfine coupling (HFC) between the paramagnetic ligand and the nitrogen atoms of the central porphyrin ring was measured. The obtained results were compared with the data for a similar, commercially available cationic porphyrin (5,10,15,20-tetrakis(*N*-methyl-4-pyridyl))porphyrin (TMPyP4) containing no bulky substituents.

EXPERIMENTAL

Materials and methods. All reagents were analytic grade Sigma-Aldrich chemicals. The solvents were purified by standard procedures. The ^{1}H and ^{13}C NMR spectra of solutions in $CDCl_3$ or CD_3OD were recorded on a Bruker MSL-300 pulse Fourier transform spectrometer. Tetramethylsilane or boron trifluoride etherate was used as an external standard. Elemental analysis for C, H, N, S was carried out on a FLASH EA 112 analyzer (Termo Finnigan, Italy). Mass spectra were measured using a liquid chromatograph. The LC system consisted of LC-20AD pumps (Shimadzu, Japan) and an autosampler connected to an LCMS-IT-TOF mass spectrometer equipped with an electrospray ionization source (Shimadzu, Japan). The spectra were obtained by direct injection without a column. Mass spectra were recorded in the *m/z* ranges of 120–700 Da for negative ionization mode and 100–700 Da for positive ionization mode. Ionization conditions: ESI voltage of 4.50 kV; carrier gas flow rate of 1.50 L/min; temperature of 200.0°C. Before analysis, the equipment was tuned (mass calibration and sensitivity testing). The electronic absorption spectra of porphyrin solutions were measured on an HACH DR-4000V instrument (Hach-Lange, USA) in the wavelength range of 320–1100 nm with a 1 nm step in quartz cells with an optical path length of 10 mm at room temperature. The compounds C_5Py

and metal complexes were described previously [10]. The porphyrin TMPyP4 (323497) was purchased from Sigma-Aldrich Chem. The structures of porphyrins are presented in Scheme 2.

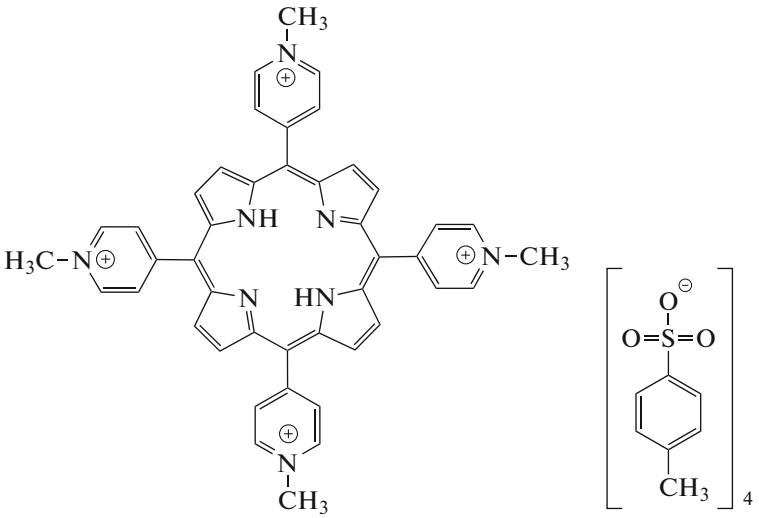

TmPyP4

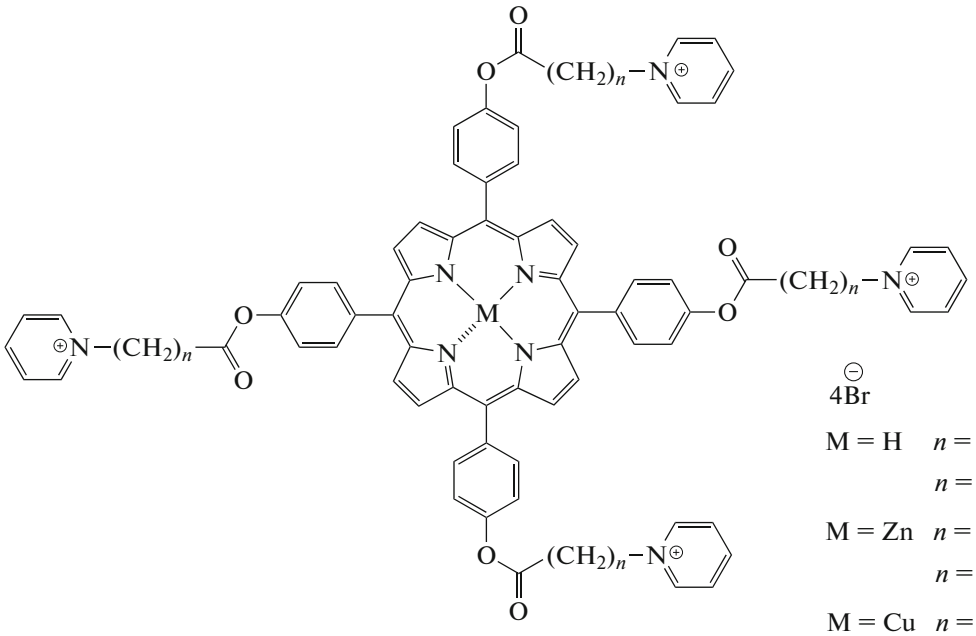

4Br

M = H $n = 3$ (C_3Py)
$n = 5$ (C_5Py)
M = Zn $n = 3$ (C_3Py-Zn)
$n = 5$ (C_5Py-Zn)
M = Cu $n = 3$ (C_3Py-Cu)
$n = 5$ (C_5Py-Cu)

Scheme 2.

Synthesis of 5,10,15,20-tetrakis(4-(4-bromo-*n*-butanoyl)oxyphenyl)porphyrin. Weighed portions of pyrrole (100 mg, 1.50 mmol) and 4-(4-bromo-*n*-butanoyl)oxybenzaldehyde (406.3 mg, 1.50 mmol) were dissolved in dichloromethane (100 mL). The reaction mixture was stirred at room temperature for 15 min, with the flask being saturated with inert gas. Then BF_3 Et_2O (20 μL, 0.15 mmol) and anhydrous ethanol (200 μL) were added. The reaction mixture was stirred for 1 h in an argon flow, and then DDQ (341 mg, 1.50 mmol) was added. After 3 h, the reaction mixture was concentrated on a rotary evaporator at a reduced pressure. The target compound was isolated by column chromatography on silica gel G60. The elution was carried out with dichloromethane with subsequent

increase in the polarity to a 40 : 1 dichloromethane–ethyl acetate system. The product was dried over P_2O_5 at a reduced pressure. The yield was 0.16 g (33%). R_f = 0.7 (dichloromethane/ethyl acetate = 40 : 1). ^{1}H NMR ($CDCl_3$; δ, ppm): 2.74 (2H, s, NH-pyrrole), 2.35–2.58 (8H, m, $OCOCH_2C\underline{H}_2$), 2.90–3.15 (8H, m, $OCOC\underline{H}_2$), 3.60–3.75 (8H, m, $C\underline{H}_2Br$), 7.52 (8H, d, J = 8.25 Hz, 3,5-(ArH)), 8.32 (8H, d., J = 8.18 Hz, 2,6-(ArH)), 8.92 (8H, s, CH-pyrrole).

Synthesis of 5,10,15,20-tetrakis(4-(4-pyridylbutanoyl)oxyphenyl)porphyrin tetrabromide (C_3Py). 5,10,15,20-Tetrakis(4-(4-bromo-*n*-butanoyl)oxyphenyl)-porphyrin (40.0 mg, 0.031 mmol) was dissolved in anhydrous pyridine (15 mL). The reaction mixture was refluxed for 3 h. The precipitate formed during the synthesis was washed with chloroform and filtered off. The chloroform extract was concentrated at a reduced pressure. The residue was dissolved in methanol and recrystallized from diethyl ether. The product was dried over P_2O_5 at a reduced pressure.

For $C_{80}H_{70}N_8O_8Br_4$

Anal. calcd., %	C, 60.43	H, 4.37	N, 7.05
Found, %	C, 60.54	H, 4.35	N, 7.12

R_f 0.2 (CH_2Cl_2 : EtOAc = 1 : 1); UV–Vis (λ_{max}, nm (logε): 415 (5.50); 513 (4.24); 547 (3.73); 589 (3.57); 645 (3.53). ^{1}H NMR (CD_3OD; δ, ppm): –2.73 (2H, s, NH), 2.53 (8H, m, $OCOCH_2C\underline{H}_2CH_2$), 2.99 (8H, m, $OCOC\underline{H}_2CH_2CH_2$), 3.34 (8H, m, $C\underline{H}_2Py$), 7.41 (8H, d, J = 8.13 Hz, 3,5-(ArH)), 8.04 (8H, d, J = 8 Hz, 2,6-(ArH)), 8.20 (8H, t, J = 7.72 Hz, 3,5-Py), 8.65–8.76 (12H, m., 4-Py + CH), 9.12 (8H, m, 2,6-pyrrole). ^{13}C NMR (CD_3OD; δ, ppm): 172.72.

Synthesis of zinc 5,10,15,20-tetrakis(4-(4-pyridylbutanoyl)oxyphenyl)porphyrin tetrabromide (C_3Py-Zn). A weighed portion of 5,10,15,20-tetrakis(4-(4-bromo-*n*-butanoyl)oxyphenyl)porphyrin (30.0 mg, 0.024 mmol) was dissolved in dichloromethane (15 mL). Then a solution (15 mL) of zinc acetate dihydrate (26.3 mg, 0.12 mmol) was added. The reaction mixture was stirred at room temperature for 3 h. The progress of the reaction was estimated from the UV–Vis spectra. Then the reaction mixture was concentrated under reduced pressure and extracted with a dichloromethane/water system. The target compound was isolated by column chromatography on silica gel G60. The elution was carried out in a 40 : 1 dichloromethane/ethyl acetate system. The product was dried over P_2O_5 at a reduced pressure. The yield was 30 mg (94%). R_f = 0.50 (dichloromethane). UV–Vis (λ_{max}, nm (logε)): 425 (5.50), 556.2 (4.18), 598.5 (3.77).

A weighed portion of zinc 5,10,15,20-tetrakis(4-(4-bromo-*n*-butanoyl)oxyphenyl)porphyrin (30 mg, 0.022 mmol) was dissolved in anhydrous pyridine (15 mL). The reaction mixture was refluxed for 3 h. The precipitate that formed during the synthesis was collected on a filter and washed with dichloromethane. The reaction mixture that dissolved in the nonpolar solvent was concentrated in vacuum. The residue was dissolved in methanol and recrystallized from diethyl ether. The target product was dried over P_2O_5 at a reduced pressure. The yield was 34.0 mg (73%).

For $C_{80}H_{68}N_8O_8Br_4Zn$

Anal. calcd., %	C, 71.98	H, 5.13	N, 8.39
Found, %	C, 71.73	H, 5.10	N, 8.46

R_f = 0.35 (methanol). R_f 0.45 (CH_3OH). R_f 0.2 (CH_2Cl_2 : EtOAc = 1 : 1); UV–Vis, λ_{max}, nm (logε): 419 (5.28); 562 (4.61); 603 (3.96). ^{1}H NMR (CD_3OD; δ, ppm): 2.03 (8H, m, $OCOCH_2C\underline{H}_2CH_2$), 3.34 (8H, m, $OCOC\underline{H}_2CH_2CH_2$), 4.80 (8H, m, $CH_2C\underline{H}_2Py$), 7.22 (8H, d, J = 8.26 Hz, 3,5-(ArH)), 7.60 (8H, d, J = 8 Hz, 2,6-(ArH)), 8.01 (8H, t, J = 7.76 Hz, 3,5-Py), 8.59–8.69 (12H, m, 4-Py + CH pyrrole), 8.89 (8H, d, J = 5.66 Hz, 2,6-Py). ^{13}C NMR (CD_3OD; δ, ppm): 172.57, 151.59, 145.82, 144.78, 139.39, 134.96, 128.43, 119.68, 119.23, 61.14, 30.21, 26.12. ESI-MS 827.23 $[M]^{2+}$.

Synthesis of copper 5,10,15,20-tetrakis(4-(4-pyridylbutanoyl)oxyphenyl)porphyrin copper tetrabromide (C_3Py-Cu). 5,10,15,20-Tetrakis(4-(4-bromo-*n*-butanoyl)oxyphenyl)porphyrin (30.0 mg, 0.024 mmol) was dissolved in dichloromethane (15 mL). Then a solution (15 mL) of copper acetate (45.7 mg, 0.251 mmol) was addded. The reaction mixture was stirred at room temperature for 3 h. The progress of the reaction was estimated from the UV–Vis spectra. Then the reaction mixture was concentrated under reduced pressure and extracted with a dichloromethane/water system. The target compound was isolated by column chromatography on silica gel G60. The elution was carried out in a 40 : 1 dichloromethane/ethyl acetate system. The product was dried over P_2O_5 at a reduced pressure. The yield was 29.1 mg (93%). R_f = 0.50 (dichloromethane). UV–Vis (λ_{max}, nm (logε)): 413 (5.45), 531(4.51).

A weighed portion of 5,10,15,20-tetrakis(4-(4-bromo-*n*-butanoyl)oxyphenyl)porphyrin copper (20 mg, 0.015 mmol) was dissolved in anhydrous pyridine (15 mL). The reaction mixture was refluxed for 3 h. The precipitate that formed during the synthesis was collected on a filter and washed with dichloromethane. The reaction mixture that dissolved in the nonpolar solvent was concentrated in vacuum. The residue was dissolved in methanol and recrystallized from diethyl ether. The target product was dried over P_2O_5 at a reduced pressure. The yield was 21 mg (85%).

For $C_{80}H_{68}N_8O_8Br_4Cu$

Anal. calcd., %	C, 72.08	H, 5.14	N, 8.41
Found, %	C, 72.20	H, 5.09	N, 8.35

R_f = 0.35 (methanol). R_f 0.60 (CH_3OH). UV–Vis (λ_{max}, nm (log ε)): 413 (5.31), 537 (4.54). ESI-MS 826.7 $[M]^{2+}$.

The ESR samples were prepared at 80 K; the cationic porphyrins were dissolved in DMF to a concentration of 15 mM. Before each measurement, the concentrated porphyrin solutions were diluted to a concentration of 250 μM, and 40-μL portions were placed in quartz tubes (with an outer diameter of 3.8 mm and an inner diameter of 2.8 mm). Before being placed in the cavity of the ESR spectrometer, the samples were shock frozen in liquid nitrogen. The laser excitation was performed using the second harmonic of a Lotis TII Nd:YAG pulsed laser (532 nm) with a repetition rate of 10 Hz. The laser output radiation was introduced through the cavity window using a system of rotating prisms. The average laser pulse power aahead of the window was 15–20 mJ; this was sufficient to excite all porphyrin molecules in the sample.

Time-resolved ESR experiments were carried out on a home-produced spectrometer based on a Bruker EMX instrument, equipped with a liquid nitrogen cooling system (77–300 K). The field step was 0.4 mT for all TR ESR spectra; 30 measurements were made at each point, 3 scans, and a power of 13 μW. The time dependence recorded in a off-resonance field (100 mT) was subtracted from each time dependence obtained in this way. The TR ESR spectra were simulated using the EasySpin Matlab package [20].

The steady-state ESR spectra were measured on a Bruker Elexsys E580 X-band ESR spectrometer equipped with a ER 4118XMD5 cavity (9.75 GHz) and an Oxford Instruments temperature controller to carry out measurements in the 20–277 K temperature range.

The ESR spectra were simulated using the EasySpin Matlab package [20].

RESULTS AND DISCUSSION

The cationic *meso*-aryl-substituted porphyrins (Scheme 2) with charged pyridinium groups were synthesized using the approach we developed previously [21]. The synthetic route to cationic porphyrins includes two steps. The first step is the Lindsay condensation of pyrrole with benzaldehydes substituted with fatty acid residues under mild conditions [22] using boron trifluoride etherate ($BF_3 \cdot Et_2O$) as the acid catalyst to give bromine-substituted porphyrin precursors. The second step includes the preparation of cationic compounds by the pyridine quaternization reaction. The use of this approach reduces the number of steps needed to obtain the target porphyrin products and facilitates the isolation and chromatographic purification of the products. The Zn(II) and Cu(II) complexes were obtained in the porphyrin precursor step in nearly quantitative yields by standard procedures. Metal complex formation was monitored using UV–Vis spectroscopy. The structures of the products formed in every step of the synthesis were confirmed by multinuclear NMR spectroscopy, UV spectroscopy, mass spectrometry, and elemental analysis.

Figure 2 shows the TR ESR spectra recorded at 80 K within 2 μs after the laser pulse. All spectra of the photoexcited triplet states for metal-free porphyrins have the same type of electron spin polarization (EEE/AAA, where A is absorption and E is emission); however, the position of lines and, hence, the parameters D and E for C_3Py and C_5Py differ from those for TMPyP4.

The parameters D and E for cationic porphyrins derived from simulated ESR spectra are presented in Table 1. According to published data, D and E for unsubstituted tetraphenylporphyrin (TPP) are 1120 and 221 MHz, respectively [17, 19]. Analysis of the results shows that the most pronounced change in D and E compared to those of TPP is observed for TMPyP4, in which the pyridinium groups are introduced directly into the porphyrin macrocycle. In this case, |D| increases by 10%, while |E| decreases 1.5-fold, which is most likely due to the decrease in the spin density delocalization in the triplet state. The introduction of pyridinium substituents via alkyl spacers does not significantly change D and E and, therefore, does not affect the triplet state configuration. This result is important, as cationic groups are introduced to ensure solubility and should not cause undesirable changes in the electronic structure.

The introduction of zinc into the porphyrins C_3Py and C_5Py induces a change in the spectral pattern and a change in the polarization type to AAA/EEE (see above). This change in the spectral pattern is characteristic of Zn-containing porphyrins and is attributable to modification of the occupancies of triplet sublevels upon the introduction of Zn. The appearance of spin–orbit coupling with the zinc ion leads to mixing of zinc *d*-orbitals with the porphyrin π-system and, consequently, the T_z sublevel is mainly populated upon the singlet–triplet (S–T) intersystem crossing in the photoexcited triplet state. Like for metal-free porphyrins, the introduction of pyridinium substituents via alkyl spacers does not significantly affect the electronic structure of the triplet state of the zinc porphyrin complex.

Copper(II) porphyrin complexes cannot be studied by time-resolved ESR due to the short lifetime of the triplet state. Therefore C_3Py-Cu(II) and C_5Py-Cu(II) were studied using steady-state ESR to measure the HFC between the paramagnetic Cu(II) center and the nitrogen centers of the porphyrin central ring.

Figure 3 shows the steady-state ESR spectra recorded at 80 K for C_3Py-Cu and C_5Py-Cu. For Cu(II)-containing porphyrins, the interaction of the unpaired electron of copper with the nuclear spin I = 3/2 (HFC) induces splitting of each line corresponding to definite orientation in the ESR spectrum into

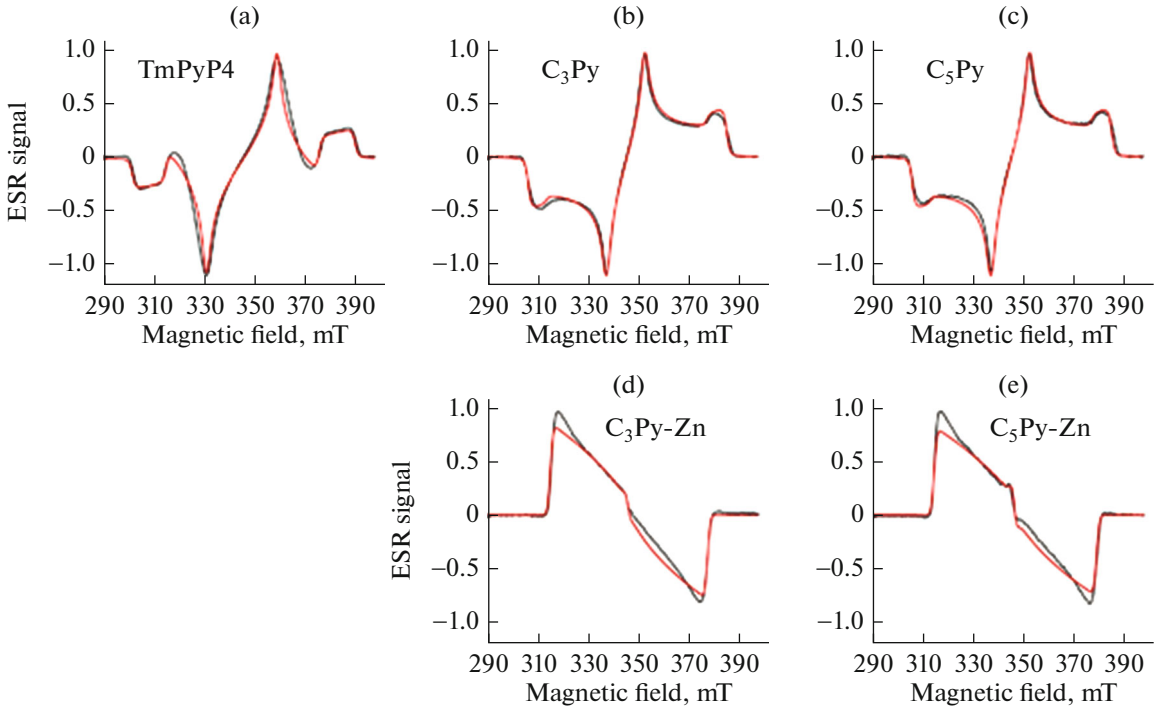

Fig. 2. TR ESR spectra of porphyrins recorded at 80 K in DMF: (a) TmPyP4, (b) C_3Py, (c) C_5Py, (d) C_3Py-Zn, (e) C_5Py-Zn. Black color shows experimental data and red color corresponds to simulation.

four lines. In addition, copper(II) ions have a considerable *g*-tensor anisotropy, which gives rise to fairly complex powder spectra with overlapping lines in the X-band. Additional interaction of the unpaired electron spin with four nitrogen atoms with $I = 1$ gives rise to additional hyperfine structure. The obtained experimental data were subjected to simulation with allowance for *g*- and HFC-tensor (A) anisotropy; the results are given in Table 2. The line broadening parameters of the ESR spectra are similar for both complexes. The HFC on porphyrin nitrogens depends on the spin density of the paramagnetic center on these nuclei and, in the point dipole approximation, it is determined by the distance between the paramagnetic center and nitrogen atoms. The simulated ESR spectra showed that the macrocycle nitrogens in C_3Py-Cu(II) and C_5Py-Cu(II) are equivalent, and the HFC tensors differ little from that of TMPyP4-Cu(II) [23].

The results obtained for C_3Py-Cu(II) and C_5Py-Cu(II) suggest that the spatial positions of the nitrogen atoms in the porphyrin macrocycle of the Cu(II) complex do not change significantly upon the introduction

Table 1. Parameters D and E for the triplet states of porphyrins determined from simulated TR ESR spectra*

Porphyrin	|D|, MHz	|E|, MHz	Relative occupancy of triplet sublevels $p_x : p_y : p_z$
C_3Py	1125	230	0.4 : 1 : 0
C_5Py	1125	230	0.4 : 1 : 0
C_3Py-Zn	890	292	0 : 0 : 1
C_5Py-Zn	925	300	0 : 0 : 1
TmPyP4	1260	155	0.65 : 1 : 0.6
TPP [17, 19]	1120	221	

* The absolute signs of D and E cannot be directly derived from the TR ESR spectra; therefore, only their absolute magnitudes are given. The error is ±5 MHz.

Table 2. Parameters of the *g*- and HFC-tensors and line broadening for copper porphyrin complexes derived from simulation of the steady-state ESR spectra using the EasySpin program package

Porphyrin	*g*-Tensor	Tensor of HFC with Cu (A_Cu), MHz	Tensor of HFC with N (A_N), MHz	Line broadening from peak to peak, mT
C_3Py-Cu	$g_{xx} = 2.054$ $g_{yy} = 2.072$ $g_{zz} = 2.211$	$A\_Cu_{xx} = 48$ $A\_Cu_{yy} = 56$ $A\_Cu_{zz} = 604$	$A\_N_{xx} = A\_N_{yy} = 52$ $A\_N_{zz} = 43$	Nonuniform (0.10), uniform (0.45)
C_5Py-Cu				Nonuniform (0.20), uniform (0.51)

of pyridinium substituents in the porphyrin core, that is, they remain equivalent.

Thus, cationic *meso*-substituted porphyrins and their Zn(II) and Cu(II) complexes were synthesized. The compounds were characterized by modern physicochemical methods. The zero-field splitting parameters of photoexcited triplet states were determined by time-resolved ESR. The pyridinium groups introduced directly into the porphyrin macrocycle were found to influence the triplet state parameters. However, the introduction of pyridinium substituents via alkyl spacers does not change substantially the triplet state configuration. The pyridinium substituents also do not disrupt the equivalence of nitrogen atoms in the porphyrin macrocycle of the Cu(II) complex.

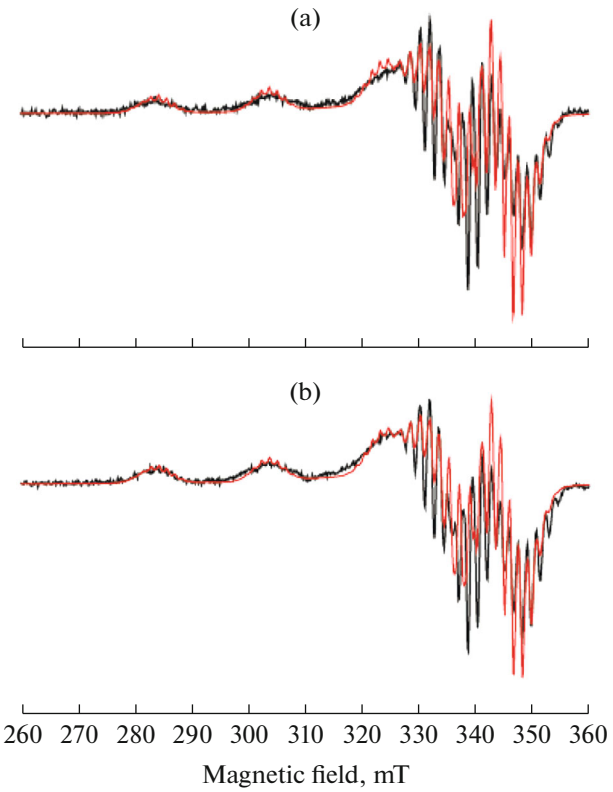

Fig. 3. X-band steady-state ESR spectra in DMF at 80 K: (a) C_3Py-Cu, (b) C_5Py-Cu. Black color shows experimental data and red color corresponds to simulation.

FUNDING

The study was supported by the Russian Science Foundation (project no. 20-73-10239).

CONFLICT OF INTEREST

The authors declare that they have no conflicts of interest.

REFERENCES

1. Shi, Y., Zhang, F., and Linhardt, R.J., *Dye. Pigment.*, 2021, vol. 188, p. 109136.
2. Wang, Z., Sun, Q., Liu, B., et al., *Coord. Chem. Rev.*, 2021, vol. 439, p. 213945.
3. Kawczyk-Krupka, A., Pucelik, B., Miedzybrodzka, A., et al., *Photodiagnosis Photodyn. Ther.*, 2018, vol. 23, p. 132.
4. Lee, J.-H., Shao, S., Cheng, K.T., et al., *J. Liposome Res.*, 2015, vol. 25, no. 2, p. 101.
5. He, M., Chen, Y., Tao, C., et al., *ACS Appl. Mater. Interfaces*, 2019, vol. 11, no. 45, p. 41946.
6. Annunzio, S.R.D., Costa, N.C.S., Mezzina, R.D., et al., *Int. J. Mol. Sci.*, 2019, vol. 20, no. 16, p. 3861.
7. Mironov, A.F., Zhdanova, K.A., and Bragina, N.A., *Russ. Chem. Rev.*, 2018, vol. 87, no. 9, p. 859.
8. Sengupta, D., Timilsina, U., Mazumder, Z.H., et al., *Eur. J. Med. Chem.*, 2019, vol. 174, p. 66.
9. Yi, X., Wang, F., Qin, W., et al., *Int. J. Nanomedicine*, 2014, p. 1347.
10. Gao, D., Guo, X., Zhang, X., et al., *Mater. Today Bio*, 2020, vol. 5, p. 100035.
11. Habermeyer, B. and Guilard, R., *Photochem. Photobiol. Sci.*, 2018, vol. 17, no. 11, p. 1675.
12. Sannikova, N.E., Timofeev, I.O., Chubarov, A.S., et al., *J. Photochem. Photobiol.*, 2020, vol. 211, p. 112008.
13. DuPont, J.I., Henderson, K.L., Metz, A., et al., *Biochim. Biophys. Acta Gen. Subj.*, 2016, vol. 1860, no. 5, p. 902.
14. Malcolm, D.E., Forbes, M.D.E., Lauren, E., et al., *Adv. Phys. Org. Chem.*, 2013, p. 1.

15. Wang, Z., Ivanov, M., Gao, Y., et al., *Chem.-A Eur. J.*, 2020, vol. 26, no. 5, p. 1091.
16. Ivanov, M.Y., Veber, S.L., Prikhod'ko, S.A., et al., *J. Phys. Chem. B*, 2015, vol. 119, no. 42, p. 13440.
17. Kay, C.W.M., *J. Am. Chem. Soc.*, 2003, vol. 125, no. 45, p. 13861.
18. Langhoff, S.R., *J. Chem. Phys.*, 1975, vol. 62, no. 1, p. 169.
19. Yamauchi, A., Fujiwara, S., Nishimura, K., et al., *J. Phys. Chem. A*, 2021, p. 4334.
20. Stoll, S. and Schweiger, A., *J. Magn. Reson.*, 2006, vol. 178, no. 1, p. 42.
21. Zhdanova, K.A., Savelyeva, I.O., Ignatova, A.A., et al., *Dye. Pigment.*, 2020, vol. 181, p. 108561.
22. Lindsey, J.S. and Hsu, H.C., *Tetrahedron Lett.*, 1986, vol. 27, no. 41, p. 4969.
23. Greiner, S.P., Rowlands, D.L., and Kreilick, R.W., *J. Phys. Chem.*, 1992, vol. 96, no. 23, p. 9132.

Translated by Z. Svitanko